

Modeling the Radial Elastic Interaction between Reinforcing Bars and Concrete

Hailing Yu, Student M. ASCE and James V. Cox, M. ASCE
Johns Hopkins University, Baltimore, MD 21218
hailing@ceexp2.ce.jhu.edu, James.Cox@jhu.edu

Abstract

The fabricated surface structures of steel and most fiber-reinforced polymer (FRP) bars produce complicated mechanical interactions with concrete. At one scale of modeling, the bar-concrete interface is idealized as smooth, and the actual interaction is homogenized over a characteristic length associated with the surface structure. To account for the elastic aspects of the mechanical interlocking, an interface with an elastic component may be introduced. The elastic modulus associated with the radial response is important in predicting the splitting failure of concrete and is the key issue of this study.

For the case of steel bars, limited experimental data suggests that the radial compliance varies with contact conditions. An analytical study has demonstrated that an “effective elastic modulus” of an interface varies with the distribution of the interface traction, but the analytical model is only valid for relatively stiff reinforcement. An overview of the extension of this work to address relatively compliant reinforcements (*e.g.*, FRP bars) is presented. For steel bars, a simple contact model combined with selected experimental data provides an approximation for the contact conditions near the ribs; this approximation can then be used to account for the effects of changing contact conditions upon the radial elastic modulus in a phenomenological bond model. Incorporating these effects into the bond model significantly improves the predicted radial responses of selected bond specimens.

Introduction

Modeling the behavior of reinforced concrete requires models for both the constituent materials and their interaction. For steel and most fiber-reinforced polymer (FRP) bars their fabricated surface structure (*e.g.*, ribs or indentations), by design, results in a complicated mechanical interaction with concrete. Although several models have been proposed to study the mechanical interaction and its effect upon structural behavior, additional work is needed to quantify the radial component of the interaction which is important in predicting splitting failures of concrete (both for steel and FRP bars). In recent years, additional experimental studies have been conducted (see *e.g.*, Gambarova *et al.* 1989, Malvar 1992, 1995, Noghabai 1995, Tepfers and Olsson 1992, and Ghandehari *et al.* 1999) that examine some aspects of the radial response. These studies provide important data for obtaining a better understanding of the underlying mechanics. Additional analytical and numerical studies are also needed to better understand and characterize the observed experimental behaviors.

The mechanical interaction between reinforcing bars and concrete, often referred to as *bond*, is generally attributed to three mechanisms - chemical adhesion, friction, and mechanical interlocking. For reinforcements with a *significant surface structure*, mechanical interlocking is the dominant mechanism affecting the bond-slip behavior. The effects of the mechanical interaction have been modeled computationally at several scales (see *e.g.*, Cox and Herrmann 1998), two of which are depicted in Fig. 1. Usually in *rib-scale* analyses either the geometry of the surface structure or its local effects (*e.g.*, a concentrated traction distribution near each rib) are explicitly modeled. In *bar-scale* analyses, the geometry of the interface is idealized as cylindrical,

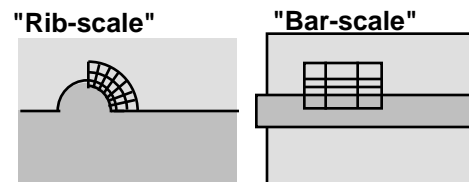


FIG. 1. Two scales of bond analysis.

and the interface traction is homogenized over a characteristic length associated with the surface structure. As such, the effects of the mechanical interlocking must be accounted for indirectly in bar-scale models. One approach to modeling the mechanical interaction at this scale is to adopt an interface idealization (see *e.g.*, De Groot *et al.* 1981, and Cox and Herrmann 1998).

While the analysis approach presented here is not tied to a particular bond model, validation of the model by Cox and Herrmann (1999) motivated this study. This bond model, combined with specimen models, adequately reproduced the experimental results from several different studies using a single calibration. (Both steel and FRP bars have now been considered.) The model was formulated within the mathematical framework of elastoplasticity, so the model components to be defined were the generalized stresses and strains, elastic moduli, yield criterion, and flow rule. The generalized stresses are the homogenized tangent (τ) and normal (σ) traction components¹ on the cylindrical interface, and the generalized strains are the corresponding work conjugate relative displacements (δ_t and δ_n , respectively) nondimensionalized by the bar diameter (D_b). The generalized stresses and strains are thus written as

$$\mathbf{Q}^T = (\tau \quad \sigma) \text{ and } \mathbf{q}^T = (\delta_t/D_b \quad \delta_n/D_b) \quad (1)$$

The strains \mathbf{q} (and relative displacements) are additively decomposed into the elastic (\mathbf{q}^e) and plastic (\mathbf{q}^p) components, and a linear relationship between the stresses and elastic strains is assumed, *i.e.* $\mathbf{Q} = \mathbf{D}^e \mathbf{q}^e$. Experimental data indicates that it is sufficient to only retain the diagonal elastic moduli giving

$$\mathbf{D}^e = \text{diag}(D_{11}^e, D_{22}^e) \quad (2)$$

D_{11}^e can be calibrated from bond test data, but very little data exists to evaluate D_{22}^e . This paper focuses on D_{22}^e for two reasons. For a model that “fully couples” the tangent and normal responses, the bond stress-slip behavior is affected by the radial response. Furthermore, the radial elastic component of the interaction is very important in predicting splitting failures of adjacent concrete.

For simplicity (and lack of experimental data) D_{22}^e for most bond models is defined to be constant. However, two unpublished tests of Malvar (1992) suggest that the radial elastic response becomes more compliant with radial dilation (*i.e.*, increasing δ_n). To account for this variation, elastoplastic coupling was recently introduced into the model of Cox and Herrmann by expressing D_{22}^e as a function of the radial plastic strain q_2^p . As a preliminary model Cox (1996) proposed a linear relationship between the interface compliance and q_2^p of the form

$$\left(D_{22}^e/E_c\right)^{-1} = k_1 + k_2 q_2^p \quad (3)$$

where E_c is Young’s modulus of concrete and k_1 and k_2 are model parameters. While the prediction of radial responses was improved by this formulation, additional justification was sought. An analytical study by Cox and Yu (1999) showed that an “effective interface compliance” increased as the radial traction became more concentrated.

The next section outlines how this analytical work can be extended to address FRP rebars (which are relatively compliant in the radial direction). To bridge the gap between the analytical work and the proposed elastoplastic coupling, the third section presents a simple “contact model” to relate q_2^p to a “contact length.”

¹ Axisymmetry is assumed in the modeling, so equivalently the traction components are referred to as the longitudinal and radial components.

Analytical Models for the Equivalent Elastic Modulus of the Interface

The analyses for studying the elastic modulus are based upon the assumptions of axisymmetry and a periodic structure along the z -axis (*i.e.*, longitudinal axis). Let s_r denote the length of one cycle of the surface structure (*e.g.*, rib spacing). To define the elastic modulus, models of the radial elastic responses of the rib- and bar-scale models are examined. A macroscopically homogeneous interface traction is considered thus reducing the analysis to that of a unit cell; see Fig. 2, where the concrete and bar are depicted as a thick-walled cylinder and cylinder, respectively. Although the rib geometry is not explicitly modeled in the rib-scale unit cell, its effect is idealized as a concentrated radial traction distribution t_n over the length L_t . For the bar-scale models an interface with elastic modulus D_{22}^e is adopted, and the key steps in characterizing D_{22}^e include: (1) defining the idealized rib- (problems *a* and *c*) and bar-scale analytical models (problems *b* and *d*) shown in Fig. 2, (2) determining σ via its static equivalence to the rib-scale traction distribution t_n , *i.e.*,

$$\sigma = \frac{1}{s_r} \int_{-L_t/2}^{L_t/2} t_n dz \quad (4)$$

(3) solving elastic problems *a–d* to obtain expressions for the elastic strain energies stored in the two systems, and (4) postulating that the two systems should store the same amounts of elastic strain energy and then equating the two energy expressions to obtain an analytical solution for D_{22}^e . For brevity details are omitted, but for problems (a) and (c) the displacements can be expressed in terms of generalized Fourier series, and series expressions can be obtained for the work done by the tractions (see *e.g.*, Cox and Yu 1999 for additional details). Since the systems are elastic, the work done by the each traction equals the strain energy stored in the body. Thus “energy equivalence” of the rib- and bar-scale systems requires

$$W_a^{t_n} + W_c^{t_n} = W_b^\sigma + W_d^\sigma \quad (5)$$

where $W_a^{t_n}$ denotes the work done by t_n in problem (a), and so on. Applying the elastic solutions and the interface definitions by Eqs. (1-2), we can express Eq. (5) as

$$W_0^{\text{con}} - \pi r_i \sum_{n=1} \alpha_n v_m^{\text{con}}(r_i) + W_0^{\text{bar}} - \pi r_i \sum_{n=1} \alpha_n v_m^{\text{bar}}(r_i) = W_0^{\text{con}} + W_0^{\text{bar}} + \pi r_i s_r \sigma^2 D_b / D_{22}^e \quad (6)$$

where $D_b = 2r_i$; the superscripts “bar” and “con” denote the bar and concrete, respectively; α_n and $v_m(r_i)$ are Fourier coefficients of t_n and $u_r(r_i)$, respectively; and W_0 is the work done by a uniformly distributed traction σ acting over the length s_r . Solving Eq. (6) for D_{22}^e gives

$$D_{22}^e = -s_r \sigma^2 D_b / \sum_{n=1} \alpha_n [v_m^{\text{con}}(r_i) + v_m^{\text{bar}}(r_i)] \quad (7a)$$

For steel bars, whose contribution to the elastic modulus can be ignored, D_{22}^e is written as

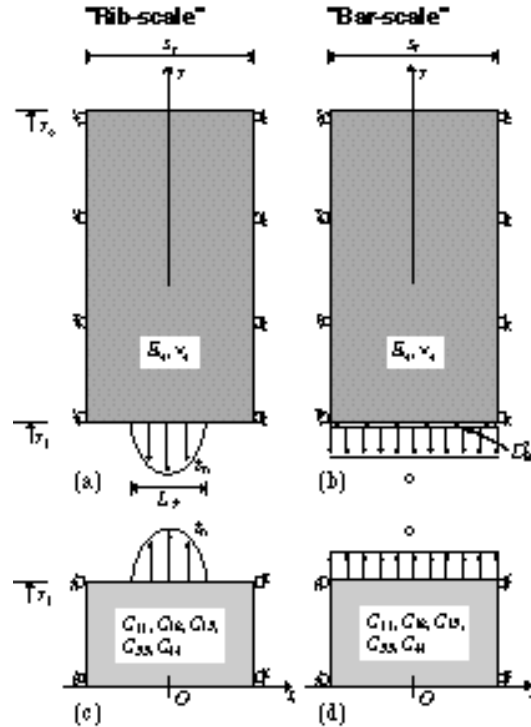


FIG. 2. Idealized analytical models.

TABLE 1. Properties of the Five Unit Cell Models for Fig. 3.

Case	L_t	D_{22}^e
a	s_r	n/a
b	1.587 mm	n/a
c	s_r	Eq. (7b) with $L_t=1.587$ mm
d	6.37 mm	n/a
e	s_r	Eq. (7b) with $L_t=6.37$ mm

$$D_{22}^e = -E_c \left/ \prod_{n=1} \right. (\alpha_n/\alpha_0)^2 \kappa(\omega_n r_i, \nu_c) \quad (7b)$$

where κ is a dimensionless function of nondimensional parameters. Clearly D_{22}^e depends on t_n (via α_n/α_0), but the concentration of the traction must be related to the bar scale model. The potential importance of D_{22}^e with respect to the radial compliance is illustrated in Fig. 3 for the Malvar specimen where $s_r=12.8$ mm and *case a* denotes a bar scale model that does not account for a reduced contact length.

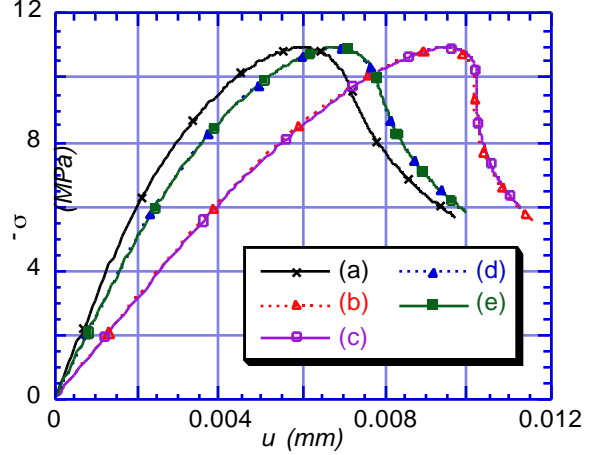


FIG. 3. Radial traction versus displacement for 5 unit cell models of a concrete cylinder subjected to an internal traction.

Contact Model

The simplified “contact model” presented in this section is only applicable to the interaction between the ribs of steel bars and concrete. The sole objective is to estimate the contact area. For steel bars that have not yielded, most of the deformation mechanism is associated with the failure of concrete. Here we limit our consideration to the accumulation of a wedge of damaged concrete on the rib face (see *e.g.*, Lutz and Gergely 1967 and Malvar 1992 for experimental evidence). Fig. 4 depicts the kinematics of the contact model where geometry gives the relations

$$p_r = h_r / \tan \varphi \quad (8a)$$

$$\delta_2^p = h_r - L_t \tan \varphi \quad (8b)$$

We assume that as concrete fails due to contact stresses a new concrete wedge surface (corresponding to φ and p_r) forms that is in contact with the concrete.

The traction components σ_w and τ_w on the actual contact surface of the concrete (Fig. 5a) can be approximated by the tractions t_n and t_t (Fig. 5b) by assuming $h_r \ll D_b$. The latter are then homogenized over s_r to give σ and τ in a manner similar to that depicted in Fig. 2.

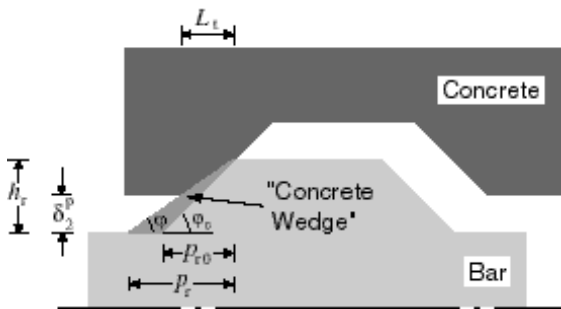


FIG. 4. Kinematics of the contact model relating contact length to plastic dilation.

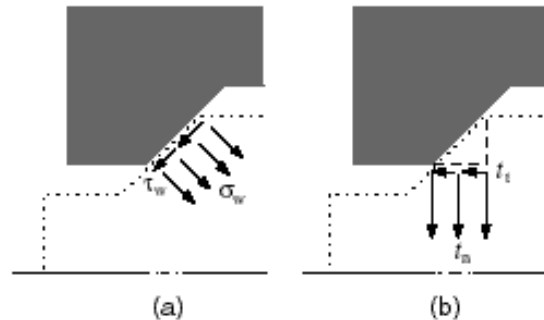


FIG. 5. Two descriptions of the “actual interface tractions.”

Uniform tractions are shown for simplicity. The relationships between the two traction descriptions are given by

$$\sigma_w = \cos\varphi (\sigma \cos\varphi - \tau \sin\varphi) s_r / L_t \quad (9a)$$

$$\tau_w = \cos\varphi (\sigma \sin\varphi + \tau \cos\varphi) s_r / L_t \quad (9b)$$

Last, we consider the material failure and slip conditions associated with the stresses. For this problem there are several obstacles to applying a multiaxial failure criterion to concrete (*e.g.*, the complete stress state is unknown). Though simplistic, we assumed that the local crushing is governed by the uniaxial condition

$$-\sigma_w \leq f_c \quad (10a)$$

where f_c is the uniaxial compressive strength of concrete. In addition, Coulomb friction is assumed to govern the slip along the actual contact interface, *i.e.*,

$$|\tau_w| \leq \mu (-\sigma_w) \quad (10b)$$

where μ is the coefficient of friction.

Elastoplastic Coupling

The analytical model for the elastic modulus and the contact model will now be combined with experimental data to obtain a form for the elastoplastic coupling (Eq. 4). Table 2 gives the experimental data for δ_2^p , σ , and τ from three bond tests when the maximum dilation first occurs (Malvar 1992). We assume $\delta_2^e \ll \delta_2^p$ so that $\delta_2^p \approx \delta_2$. At this state, we also assume that both crushing and sliding occur on the interface; *i.e.*, inequalities (10) are equalities. Given the data in Table 2, there are six equations (8-10) in six unknowns (φ , p_r , L_t , σ_w , τ_w , μ), where μ has been treated initially as an unknown. Solving the equations for each of the three tests gives values for μ of 0.554, 0.549 and 0.550, respectively. These values are surprisingly consistent for such a simple model and fall within the range of some reported experimental measurements: [0.45,0.70] (Idun and Darwin 1995). The results also give values of L_t for each δ_2^p which can be used with Eq. (7b) to relate D_{22}^e and q_2^p . Fig. 6 shows the resulting affine models (Eq. 3) fit to the experimental data for two traction distributions. The slope of the line (k_2) is not strongly dependent on the distribution type, but the negative intercept for the uniform distribution is not physically meaningful. The model based upon a cosine distribution is adopted for this study; the calibration parameters are $k_1=0.034$ and $k_2=27$. Incorporating these results into the bond model of Cox and Herrmann (1998) has significantly improved the predicted radial responses of different specimens (see *e.g.*, Fig. 7).

TABLE 2. Experimental Data

	δ_2^p (mm)	σ (MPa)	τ (MPa)
Test 6	0.512	-3.45	5
Test 8	0.135	-17.2	14
Test 10	0.029	-31	22

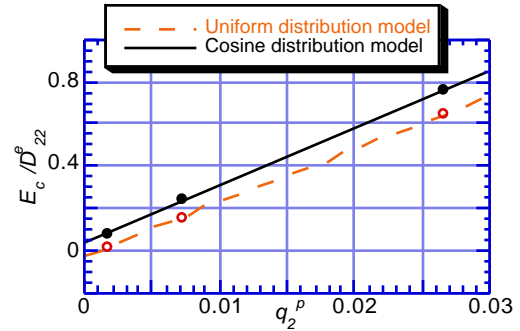


FIG. 6. Elastic compliance as a function of the generalized plastic dilation.

Conclusions

(1) An analytical expression for D_{22}^e which characterizes the radial elastic response of an interface is obtained by applying “static and energy equivalence measures” to the rib- and bar-scale analytical models. Including this elastic modulus in an interface model may

account for some aspects of the local interaction that are not explicitly characterized in larger-scale modeling.

(2) A simple “contact model” was presented to relate the contact length to the plastic dilation in the model of Cox and Herrmann. For three bond tests, the model is consistent with the experimental data, but additional experimental data is needed.

(3) Combining the analytical model for D_{22}^c with the “contact model” provides an analytical basis for the proposed elastoplastic coupling and the associated model parameters. Improvements in the predicted radial responses of bond specimens are obtained by incorporating elastoplastic coupling into the model.

Acknowledgments

Support for this study by the National Science Foundation (grant no. CMS-9872609) and the Naval Facilities Engineering Service Center (contract no. N0024498P0366) are gratefully acknowledged.

References

- Cox, J.V. (1996). “Elastic moduli of a bond model for reinforced concrete,” *Proc., 11th ASCE engineering mechanics specialty conference*, 84-87.
- Cox, J.V., and Herrmann, L.R. (1998). “Development of a plasticity bond model for reinforced concrete,” *Mechanics of Cohesive-frictional Materials*, 3, 155-180.
- Cox, J.V., and Herrmann, L.R. (1999). “Validation of a plasticity bond model for reinforced concrete,” accepted for publication, *Mechanics of Cohesive-Frictional Materials*.
- Cox, J.V., and Yu, H. (1999). “A micromechanical analysis of the radial elastic response associated with sender reinforcing elements within a matrix,” accepted for publication, *Journal of Composite Materials*.
- De Groot, A.K., Kusters, G.M.A., and Monnier, T. (1981). “Numerical modeling of bond-slip behavior,” Heron, 26-1b, I.B.B.C. Institute TNO, Delft, Netherlands.
- Gambarova, P.G., Rosati, G.P., and Zasso, B. (1989). “Steel-to-concrete bond after concrete splitting: test results,” *Materials and Structures*, International Association of Testing and Research, 22(127), 35-47.
- Ghandehari, M., Krishnaswamy, S., and Shah, S. (1999). “Technique for evaluating kinematics between rebar and concrete,” *Journal of Engineering Mechanics*, 125(2), 234-241.
- Idun, E.K., and Darwin, D. (1995). “Improving the development characteristics of steel reinforcing bars,” *SM Report No. 41*, University of Kansas Center for Research, Lawrence, Kansas.
- Lutz, L.A., and Gergely, P. (1967). “Mechanics of bond and slip of deformed bars in concrete,” *ACI Journal*, 64, 711-721.
- Malvar, L.J. (1992). “Bond of reinforcement under controlled confinement,” *ACI Materials Journal*, 89(6), 593-601.
- Malvar, L.J. (1995). “Tensile and bond properties of GFRP reinforcing bars,” *ACI Materials Journal*, 92(3), 276-285.
- Noghabai, K. (1995). “Splitting of concrete covers - a fracture mechanics approach,” *Fracture Mechanics of Concrete Structures, Proc. FRAMCOS-2*, 1575-1584.
- Tepfers and Olson (1992). “Ring Test for Evaluation of Bond Properties of Reinforcing Bars,” *Bond in Concrete, Proc. of the Int. Conf.*, CEB, pp. 1.89-1.99.

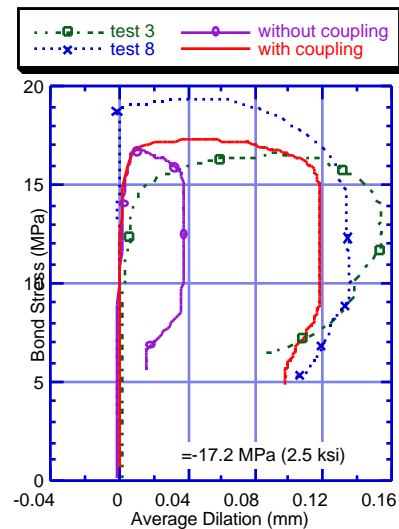


FIG. 7. Radial response predictions for Malvar test.